Nuclear Engineering and Technology 56 (2024) 141–146

Contents lists available at ScienceDirect

Nuclear Engineering and Technology

journal homepage: www.elsevier.com/locate/net

Original Article

Comparison of event tree/fault tree and convolution approaches in calculating station blackout risk in a nuclear power plant

Man Cheol Kim

School of Energy Systems Engineering, Chung-Ang University, 84 Heukseok-ro, Dongjak-gu, Seoul, 06974, South Korea

ARTICLE INFO

Keywords:
Probabilistic safety assessment
Nuclear power plant
Station blackout
Conditional core damage probability
Mathematical modeling

ABSTRACT

Station blackout (SBO) risk is one of the most significant contributors to nuclear power plant risk. In this paper, the sequence probability formulas derived by the convolution approach are compared with those derived by the conventional event tree/fault tree (ET/FT) approach for the SBO situation in which emergency diesel generators fail to start. The comparison identifies what makes the ET/FT approach more conservative and raises the issue regarding the mission time of a turbine-driven auxiliary feedwater pump (TDP), which suggests a possible modeling improvement in the ET/FT approach. Monte Carlo simulations with up-to-date component reliability data validate the convolution approach. The sequence probability of an alternative alternating current diesel generator (AAC DG) failing to start and the TDP failing to operate owing to battery depletion contributes most to the SBO risk. The probability overestimation of the scenario in which the AAC DG fails to run and the TDP fails to operate owing to battery depletion contributes most to the SBO risk overestimation determined by the ET/FT approach. The modification of the TDP mission time renders the sequence probabilities determined by the ET/FT approach more consistent with those determined by the convolution approach.

1. Introduction

Station blackout (SBO) refers to the loss of all alternating current (AC) power sources in a nuclear power plant (NPP) caused by the loss of offsite power (LOOP) followed by the failure of emergency diesel generators (EDGs). Under an SBO situation, an alternative AC power source such as an AAC DG (Alternative AC Diesel Generator) is used to maintain the NPP in a safe state. If decay heat cannot be removed by providing feedwater to the steam generators (SGs) with motor-driven auxiliary feedwater pumps, in short, motor-driven pumps (MDPs), or turbine-driven auxiliary feedwater pumps, in short, turbine-driven pumps (TDPs), the integrity of the reactor core may be challenged. When all AC power sources are not available, TDPs operate with direct current (DC) power from Class-1E DC batteries until the batteries deplete. Many probabilistic safety assessments (PSAs) have identified SBO risk as one of the most significant contributors to the overall risk of an NPP.

The SBO rule (10 CFR 50.63) [1] requires each NPP to be able to withstand an SBO event, and Regulatory Guide 1.155 [2] describes an acceptable method to comply with the regulation by the United States Nuclear Regulatory Commission. NUREG/CR-2989 [3], NUREG/CR-3226 [4], NUREG-1032 [5], and NUREG/CR-6890 [6] are some of the SBO risk studies. To properly address time dependencies in calculating the SBO risk, the convolution integrals (also known as convolution method and convolution methodology) are used in studies such as IAEA-TECDOC-593 [7], Schroeder and Buell [8], Rodi [9], Knudsen et al. [10], and Degonish [11]. The author's previous publication [12] systematically identifies SBO sequences and the associated time-dependent dependencies by differentiating fail-to-start and fail-to-run failures of an alternative AC power source and a TDP.

The purpose of this paper is to validate the sequence probability formulas derived by the convolution approach with a Monte Carlo simulation and to compare it with the conventional event tree/fault tree (ET/FT) approach to identify the amount of overestimation involved in the ET/FT approach.

For the SBO situations caused by the LOOP followed by the fail-to-start failures of EDGs, Section 2 identifies possible sequences with the ET/FT and convolution approaches. Section 3 compares the sequence probability formulas derived by the ET/FT and convolution approaches with a discussion on the mission time of the TDP. Section 4 validates the sequence probability formulas derived by the convolution approach with a Monte Carlo simulation and numerically compares the results of the ET/FT and convolution approaches. Section 5 provides the conclusion of this paper.

E-mail address: charleskim@cau.ac.kr.

https://doi.org/10.1016/j.net.2023.09.018
Received 6 February 2023; Received in revised form 12 June 2023; Accepted 13 September 2023
Available online 14 September 2023

2. SBO sequences determined by the ET/FT and convolution approaches

The author's previous publication [12] explained the station blackout sequences considered in the ET/FT and the convolution approaches in the form of event trees. In this paper, these event trees are revised with new notations explained in Section 3.

Fig. 1 describes the ET/FT approach for considering AAC DG and TDP failures after an SBO in the form of an event tree. An example of such an approach is the PSA model for the Advanced Power Reactor 1400 [13]. Fig. 1 is intended to conceptually describe how the failures of AAC DG, TDP, and AC power recovery are considered in the conventional ET/FT approach. The full event tree in practical PSA models include more details after the occurrence of an SBO.

An SBO can be properly managed if the AAC DG or the TDP successfully starts and operates during mission time. The ET/FT approach did not distinguish the fail-to-start and fail-to-run failure modes of the AAC DG and the TDP. Conservative assumptions are used where time dependency cannot be properly considered.

In engineering, the term convolution is widely used to refer to the calculation of a new distribution by combining two existing distributions. For example, in seismic probabilistic risk assessment, the seismic risk is calculated by convolving hazard and fragility curves. The term convolution has also been used for the risk calculation by combining the EDG failure time and offsite power recovery distributions [7–11].

Fig. 2 describes how event sequences are identified in the convolution approach with consideration of the failures of an AAC DG and a TDP after an SBO also in the form of an event tree. For mathematical modeling, it is necessary to distinguish the fail-to-start and fail-to-run failure modes of the AAC DG and the TDP so that the time dependency relations can be properly considered.

There are six core damage sequences: four sequences depending on how the AAC DG and TDP fail and two sequences for the battery depletion while the TDP operates without failure. In Section 3, the mathematical formulas for the six sequences are developed.

Figs. 1 and 2 describe how significant core damage sequences with time dependency are identified. For Figs. 1 and 2 to be used in a PSA, more details must be included such as the supporting systems for the EDGs, AAC DG, and TDP, secondary heat removal by using atmospheric dump valves or main steam safety valves, and accident management after the recovery of AC power.

3. Mathematical formulas for conditional core damage probabilities

In this paper, it is assumed that an SBO is caused by a LOOP and the start failures of the EDGs. To define the modeling parameters for different components consistently and concisely, the modeling parameters and subscripts are first defined. A probability is denoted as p, a failure rate is denoted as λ, and a probability density function and a cumulative distribution function are denoted as $f(t)$ and $F(t)$, respectively. A reliability function is denoted as $R(t)$, and subscripts 'A' and 'T' are used for AAC DG and TDP, respectively, while subscripts 'S' and 'R' are used for fail-to-start and fail-to-run failure modes, respectively. For example, subscript 'AS' implies the AAC DG's fail-to-start failure mode. p_{AS} and $f_{TR}(t)$ are the probability that the AAC DG fails to start and the probability density function of a TDP fail-to-run occurrence, respectively.

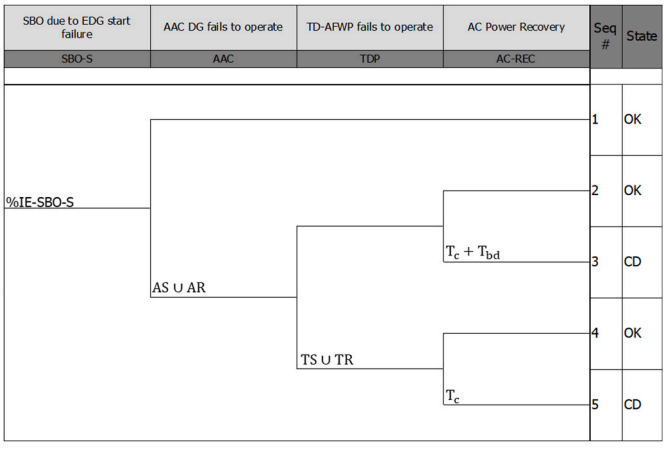

Fig. 1. Conventional consideration of AAC DG and TDP failures in the ET/FT approach.

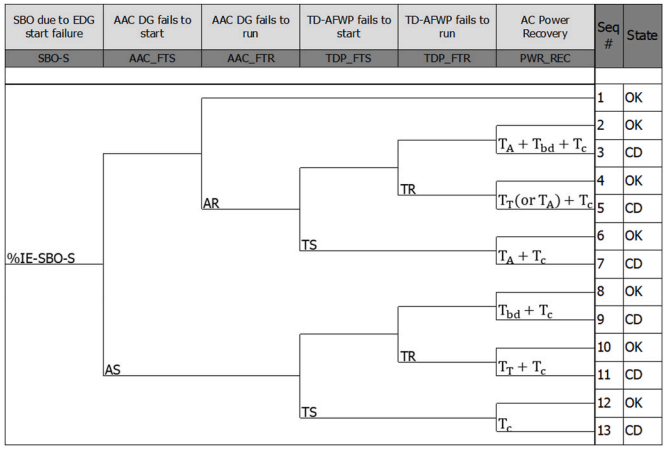

Fig. 2. Proposed consideration of AAC DG and TDP failures in the convolution approach.

Table 1 provides the notations and their descriptions used in the mathematical modeling with the numerical data for the example in Section 4. Failure probabilities and failure rates are from NUREG/CR-6928 (2020 update) [14,15]. The time-related parameters are plant-specific and should be determined based on a thermal-hydraulic analysis, the scope of the PSA, and the capacity of the Class-1E DC batteries. For the example in Section 4, typical values are assumed.

The available time for AC power recovery is the sum of the time the AAC DG has run, the time the TDP has run, and T_c. When the AAC DG or TDP fails to start, the time the component has run becomes zero.

For fail-to-run failures, a failure rate is assumed constant, and therefore the time to failure follows an exponential distribution. The probability density function, cumulative distribution function, and reliability function are, respectively,

$$f(t) = \lambda e^{-\lambda t} \tag{1}$$

Table 1
The notations and their descriptions used in the mathematical modeling with numerical data for the example in Section 4.

Notation	Description	Numerical data	
p_{AS}	the probability that the AAC DG fails to start	2.94E-02	
λ_{AR}	the failure rate of the AAC DG	1.13E-03	h^{-1}
p_{TS}	the probability that a TDP fails to start	5.32E-03	
λ_{TR}	the failure rate of a TDP	6.35E-03	h^{-1}
T_c	the time to core damage after the failure of the AAC DG and TDP	1	h
T_{bd}	the time required to deplete Class-1E DC batteries	4	h
T_m	the mission time	24	h

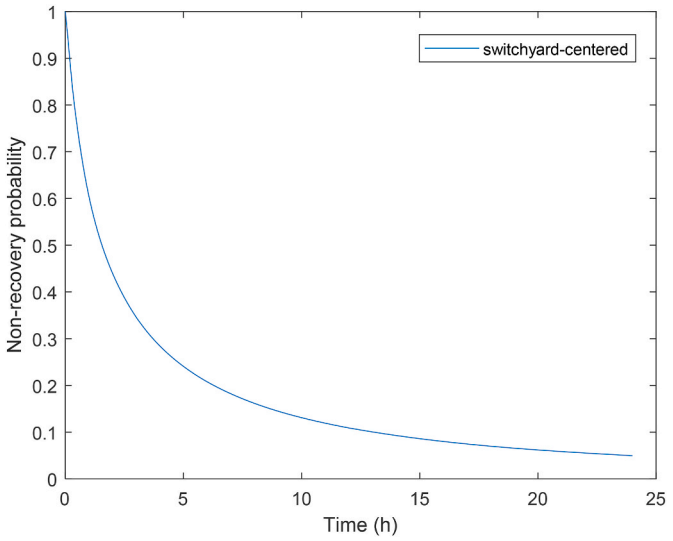

Fig. 3. Probability of non-recovery of AC power as a function of time ($p_{NRAC}(t)$) used in the example.

$$F(t) = \int_0^t f(\tau)d\tau = 1 - e^{-\lambda t} \tag{2}$$

$$R(t) = 1 - F(t) \tag{3}$$

The probability distribution for the non-recovery of AC power before t is assumed to follow a lognormal distribution as

$$p_{NRAC}(t) = 1 - \int_0^t \frac{1}{\sqrt{2\pi}\sigma x} e^{-\frac{1}{2}\left(\frac{\ln x - \mu}{\sigma}\right)^2} dx \tag{4}$$

where μ and σ are the mean and standard deviation of the natural logarithms of the data, respectively. The switchyard-centered LOOP data in NUREG/CR-6890 (2020 Update) [16,17] are used in the example in Section 4 (Fig. 3).

3.1. ET/FT approach without consideration of time dependencies

For a comparison with the mathematical formulas considering the time dependencies in an SBO situation, the mathematical formulas in the ET/FT approach without the consideration of the time dependencies are presented in this section. To compare each core damage sequence probability, the core damage sequences in Fig. 1 are divided into more specific sequences in Fig. 2. The sequence probability formulas in the ET/FT approach are derived as follows:

When both the AAC DG and TDP fail to start,

$$P_{AS,TS} = p_{AS} \cdot p_{TS} \cdot p_{NRAC}(T_c) \tag{5}$$

$$P_{AS,TR} = p_{AS} \cdot (1-p_{TS}) F_{TR}(T_m) \cdot p_{NRAC}(T_c) = p_{AS} \cdot (1-p_{TS}) \left(1 - e^{-\lambda_{TR} T_m}\right) \cdot p_{NRAC}(T_c) \tag{6}$$

When the AAC DG fails to start and the TDP becomes unable to operate owing to battery depletion,

$$\begin{aligned} P_{AS,BD} &= p_{AS} \cdot (1-p_{TS})(1 - F_{TR}(T_m)) \cdot p_{NRAC}(T_{bd} + T_c) \\ &= p_{AS} \cdot (1-p_{TS}) e^{-\lambda_{TR} T_m} \cdot p_{NRAC}(T_{bd} + T_c) \end{aligned} \tag{7}$$

When the AAC DG fails to run and the TDP fails to start,

$$P_{AR,TS} = (1-p_{AS}) F_{AR}(T_m) \cdot p_{TS} \cdot p_{NRAC}(T_c) = (1-p_{AS}) \left(1 - e^{-\lambda_{AR} T_m}\right) \cdot p_{TS} \cdot p_{NRAC}(T_c) \tag{8}$$

When the AAC DG and TDP fail to run,

$$\begin{aligned} P_{AR,TR} &= (1-p_{AS}) F_{AR}(T_m) \cdot (1-p_{TS}) F_{TR}(T_m) \cdot p_{NRAC}(T_c) \\ &= (1-p_{AS}) \left(1 - e^{-\lambda_{AR} T_m}\right) \cdot (1-p_{TS}) \left(1 - e^{-\lambda_{TK} T_m}\right) \cdot p_{NRAC}(T_c) \end{aligned} \tag{9}$$

When the AAC DG fails to run and the TDP becomes unable to operate owing to battery depletion,

$$\begin{aligned} P_{AR,BD} &= (1-p_{AS}) F_{AR}(T_m) \cdot (1-p_{TS}) [1 - F_{TR}(T_m)] \cdot p_{NRAC}(T_{bd} + T_c) \\ &= (1-p_{AS}) F_{AR}(T_m) \cdot (1-p_{TS}) R_{TR}(T_m) \cdot p_{NRAC}(T_{bd} + T_c) \\ &= (1-p_{AS}) \left(1 - e^{-\lambda_{AR} T_m}\right) \cdot (1-p_{TS}) e^{-\lambda_{TR} T_m} \cdot p_{NRAC}(T_{bd} + T_c) \end{aligned} \tag{10}$$

The conditional core damage probability (CCDP) for an SBO caused by EDGs' failure-to-start is calculated as the sum of the six sequence probabilities in Eqs. (5)–(10). In Fig. 1, Sequence 5 includes $P_{AS,TS}$, $P_{AS,TR}$, $P_{AR,TS}$, and $P_{AR,TR}$, while Sequence 3 includes $P_{AS,BD}$ and $P_{AR,BD}$.

3.2. Convolution approach with consideration of time dependencies

In the author's previous publication [12], the mathematical formulas that consider the time dependencies are derived. In this section, the mathematical formulas are presented in a different form so that each formula corresponds to a sequence in Fig. 2. Note that the new notations also apply.

In Fig. 2, there are six core damage sequences: sequences 3, 5, 7, 9, 11, and 13. The mathematical formulas for the sequence probabilities are presented below.

When both the AAC DG and TDP fail to start,

$$P_{AS,TS} = p_{AS} \cdot p_{TS} \cdot p_{NRAC}(T_c) = p_{AS} \cdot p_{TS} \cdot p_{NRAC}(T_c) \tag{11}$$

When the AAC DG fails to start and the TDP fails to run,

$$\begin{aligned} P_{AS,TR} &= p_{AS}(1-p_{TS}) \int_0^{T_{bd}} f_{TR}(t) p_{NRAC}(t + T_c) dt \\ &= p_{AS}(1-p_{TS}) \int_0^{T_{bd}} \lambda_{TR} e^{-\lambda_{TR} t} p_{NRAC}(T_c) dt \end{aligned} \tag{12}$$

When the AAC DG fails to start and the TDP becomes unable to operate owing to battery depletion,

$$\begin{aligned} P_{AS,BD} &= p_{AS}(1-p_{TS}) \int_{T_{bd}}^{\infty} f_{TR}(t) p_{NRAC}(T_{bd} + T_c) dt \approx p_{AS} \int_{T_{bd}}^{\infty} f_{TR}(t) p_{NRAC}(T_{bd} + T_c) dt = p_{AS} \cdot (1-p_{TS})(1 - F_{TR}(T_{bd})) \cdot p_{NRAC}(T_{bd} + T_c) \\ &= p_{AS} \cdot (1-p_{TS}) e^{-\lambda_{TR} T_{bd}} \cdot p_{NRAC}(T_{bd} + T_c) \end{aligned} \tag{13}$$

When the AAC DG fails to start and the TDP fails to run,

When the AAC DG fails to run and the TDP fails to start,

$$P_{AR,TS} = (1-p_{AS})\int_0^{T_m} f_{AR}(t)\cdot p_{TS}\cdot p_{NRAC}(t+T_c)dt = (1-p_{AS})p_{TS}\int_0^{T_m}\lambda_{AR}e^{-\lambda_{AR}t}\cdot p_{NRAC}(t+T_c)dt \tag{14}$$

When both the AAC DG and TDP fail to run,

$$\begin{aligned}P_{AR,TR} = (1-p_{AS})(1-p_{TS})\Bigg[&\int_0^{T_m-T_{bd}}\\ &\times\int_{t_A}^{t_A+T_{bd}} f_{AR}(t_A)f_{TR}(t_T)p_{NRAC}(t_T+T_c)dt_Tdt_A + \int_{T_m-T_{bd}}^{T_m}\\ &\times\int_{t_A}^{T_m} f_{AR}(t_A)f_{TR}(t_T)p_{NRAC}(t_T+T_c)dt_Tdt_A + \int_0^{T_m}\\ &\times\int_{t_T}^{T_m} f_{TR}(t_T)f_{AR}(t_A)p_{NRAC}(t_A+T_c)dt_Adt_T\Bigg] = (1-p_{AS})(1-p_{TS})\Bigg[\int_0^{T_m-T_{bd}}\\ &\times\int_{t_A}^{t_A+T_{bd}}\lambda_{AR}e^{-\lambda_{AR}t_A}\cdot\lambda_{TR}e^{-\lambda_{TR}t_T}\cdot p_{NRAC}(t_T+T_c)dt_Tdt_A + \int_{T_m-T_{bd}}^{T_m}\\ &\times\int_{t_A}^{T_m}\lambda_{AR}e^{-\lambda_{AR}t_A}\cdot\lambda_{TR}e^{-\lambda_{TR}t_T}\cdot p_{NRAC}(t_T+T_c)dt_Tdt_A + \int_0^{T_m}\\ &\times\int_{t_T}^{T_m}\lambda_{TR}e^{-\lambda_{TR}t_T}\cdot\lambda_{AR}e^{-\lambda_{AR}t_A}\cdot p_{NRAC}(t_T+T_c)dt_Adt_T\Bigg]\end{aligned} \tag{15}$$

When the AAC DG fails to run and the TDP becomes unable to operate owing to battery depletion,

$$\begin{aligned}P_{AR,BD} &= (1-p_{AS})(1-p_{TS})\cdot\left[\int_0^{T_m-T_{bd}} f_{AR}(t_A)\cdot\left(\int_{t_A+T_{bd}}^{\infty} f_{TR}(t_T)dt_T\right)\cdot p_{NRAC}(t_A+T_{bd}+T_c)dt_A\right]\\ &= (1-p_{AS})(1-p_{TS})\int_0^{T_m-T_{bd}} f_{AR}(t_A)\cdot(1-F_{TR}(t_A+T_{bd}))\cdot p_{NRAC}(t_A+T_{bd}+T_c)dt_A\\ &= (1-p_{AS})(1-p_{TS})\int_0^{T_m-T_{bd}}\lambda_{AR}e^{-\lambda_{AR}t_A}\cdot e^{-\lambda_{TR}(t_A+T_{bd})}\cdot p_{NRAC}(t_A+T_{bd}+T_c)dt_A\end{aligned} \tag{16}$$

The CCDP for an SBO caused by EDGs' failure-to-start is calculated as the sum of the six sequence probabilities in Eqs. (11)–(16).

3.3. Discussion

After the occurrence of an SBO, the operation of the AAC DG or TDP is necessary until AC power is recovered or the plant is in a safe state. A finite mission time is assigned after which the plant is assumed to be in a safe state. As the mission time becomes increasingly longer, the CCDP determined by the ET/FT method approaches $p_{NRAC}(T_c)$, whereas the CCDP determined by the convolution method approaches an asymptotic value with the consideration of the exponential decrease in the probability of non-recovery of AC power. The convolution approach provides a more natural way of considering the mission time of the AAC DG and TDP.

3.4. Possible modeling improvement in the ET/FT approach

The comparison between the sequence probability formulas derived by the ET/FT and convolution approaches identifies a TDP mission time issue. In the ET/FT approach, the fail-to-run failure of a TDP is modeled as an independent basic event, and the mission time of a TDP is also assumed to be T_m. This is because either the MDPs or TDPs must operate up to T_m to provide feedwater to the SGs, and therefore the mission time for both the MDPs and TDPs is assigned as T_m. The same basic event for TDP fail-to-run failure is combined with both the AAC DG fail-to-start failure and AAC DG fail-to-run failure without distinguishing between the two failures, as shown in Fig. 1. As a result, the mission time of the TDP for fail-to-run failure when the AAC DG fails to start also becomes T_m as shown in Eq. (7).

However, when the AAC DG fails to start, the TDP is only operable for the time until the batteries deplete (T_{bd}), which is usually less than T_m. After the successful operation of a TDP up to T_{bd}, the available time for AC power recovery should be assigned as $T_{bd}+T_c$; instead, it is assigned as T_c in the ET/FT approach because the TDP does not operate up to T_m. The same logic also applies when the AAC DG fails to run, in which the TDP is only operable for an additional T_{bd} after the failure of the AAD DG. Therefore, it is suggested to modify the TDP mission time from T_m to T_{bd} in the ET/FT approach.

In the proposed approach, the fail-to-start and fail-to-run failures of the AAC DG are distinguished, as illustrated in Fig. 2. This distinction allows the use of T_{bd} in Eq. (13) and T_m in Eq. (15).

When both the AAC DG and TDP fail to start, Eqs. (5) and (11) for $P_{AS,TS}$ in both the ET/FT and convolution approaches are the same. This is because no time dependency is involved in the situation.

When time dependencies are involved, the ET/FT approach adopts conservative assumptions, and therefore the probabilities calculated with the ET/FT approach are greater than those calculated with the convolution approach, except for $P_{AS,BD}$. If the TDP does not fail to start, it will either fail to run or continue to run until the battery is depleted. Therefore, the sum of $P_{AS,TR}$ and $P_{AS,BD}$ remains constant. The conservative assumption (the assignment of T_m as the mission time of the TDP) results in a conservative estimate of $P_{AS,TR}$, which leads to smaller estimates of $P_{AS,BD}$ in the ET/FT approach. If the mission time of the TDP is modified from T_m to T_{bd} in Eqs. (6) and (7), Eqs. (7) and (13) for $P_{AS,BD}$ in the ET/FT and convolution approaches become the same.

4. Validation and comparison with numerical results

In this section, the sequence probability formulas in Eqs. (11)–(16) are validated with a Monte Carlo simulation by using the numerical results. In addition, the numerical results of the ET/FT and convolution approaches are compared by applying up-to-date reliability data.

Table 2
Numerical results from the ET/FT approach, convolution approach, and Monte Carlo simulation.

No.	Probability	Sequence in Fig. 1	Sequence in Fig. 2	ET/FT approach	Convolution approach	Monte Carlo simulation
1	$P_{AS,TS}$	5	13	9.46E-05	9.46E-05	9.37E-05
2	$P_{AS,TR}$	5	11	0.002499	0.000271	2.71E-04
3	$P_{AS,BD}$	3	9	0.006041	0.006859	6.87E-03
4	$P_{AR,TS}$	5	7	8.35E-05	2.10E-05	2.10E-05
5	$P_{AR,TR}$	5	5	0.002207	0.000238	2.37E-04
6	$P_{AR,BD}$	3	3	0.005336	0.002058	2.06E-03
	$CCDP_{SBO\text{-}S}$			1.63E-02	9.54E-03	9.55E-03

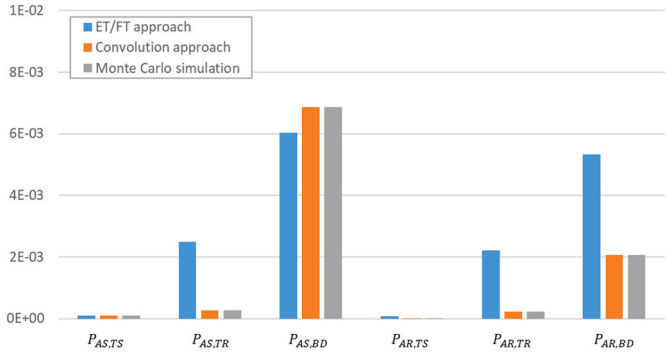

Figure 4 Comparison of numerical results between the ET/FT approach, convolution approach, and Monte Carlo simulation

Fig. 4. Comparison of numerical results between the ET/FT approach, convolution approach, and Monte Carlo simulation.

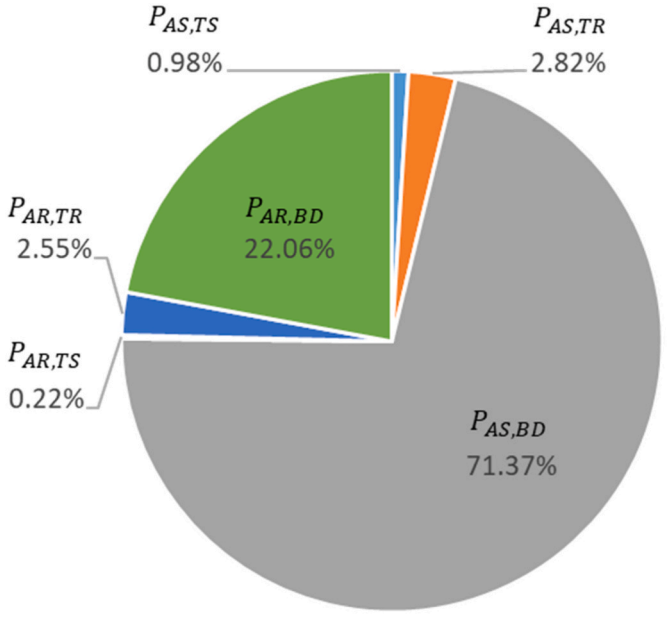

Fig. 5. SBO CCDP contribution of sequence probabilities (calculated with the convolution approach).

4.1. Validation and comparison

The numerical data in Table 1 are applied to the ET/FT approach in Eqs. (5)–(10), the convolution approach in Eqs. (11)–(16), and the Monte Carlo simulation. The failure-on-demand and failure rate data are from NUREG/CR-6928 (2020 update). The time-related data (mission time, battery depletion time, and time to core damage after the failures of the AAC DG and TDP) are assumed with typical values in nuclear power plants. The probability of non-recovery of AC power is from NUREG/CR-6890 (2020 update).

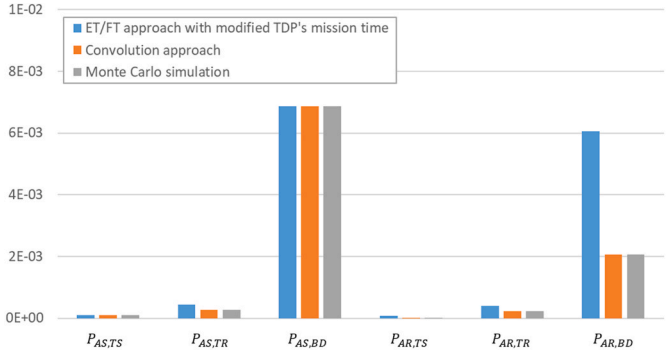

Fig. 6. Comparison of numerical results between the ET/FT approach with the modified TDP mission time, convolution approach, and Monte Carlo simulation.

In the Monte Carlo simulation, random numbers are generated to determine whether each AAC DG and TDP fails to start or not. If the AAC DG or TDP does not fail to start, the time that each of the AAC DG and TDP fails to run and the time of AC power recovery are sampled and then compared to determine whether AC power is recovered before the integrity of the reactor core is challenged. A total of 10^8 simulations were performed and the six sequence probabilities were estimated.

Table 2 shows the numerical results from the ET/FT approach, convolution approach, and Monte Carlo simulation. Fig. 4 compares the numerical results from the three approaches. The convolution approach results are in good agreement with the Monte Carlo simulation results with errors of less than 1% for the six sequence probabilities.

The sequence probabilities calculated with the ET/FT approach are greater than those calculated with the convolution approach (and Monte Carlo simulation) except for $P_{AS,BD}$, as discussed in Section 3.3. The $P_{AS,TR}$ and $P_{AR,TR}$ of the ET/FT approach are 9.21 and 9.28 times greater than those of the convolution approach, respectively. The exception of $P_{AS,BD}$ and the large overestimation of $P_{AS,TR}$ and $P_{AR,TR}$ are caused by the assignment of a conservative mission time for the TDP. This is further discussed in Section 4.2.

The difference in $P_{AR,BD}$ contributes significantly to the difference in the CCDPs between the ET/FT and convolution approaches, followed by the differences in $P_{AS,TR}$ and $P_{AR,TR}$. In other words, the overestimation of $P_{AR,BD}$ contributes significantly to the overestimation of the CCDP by the ET/FT approach, followed by the overestimation of $P_{AS,TR}$ and $P_{AR,TR}$.

If the mission time (T_m) is very large, the CCDPs by the ET/FT and convolution approaches are 0.6045 ($=p_{NRAC}(T_c)$) and 0.0115, respectively. Therefore, the ET/FT approach significantly overestimates the CCDP.

Fig. 5 shows the contributions of the sequence probabilities to the SBO CCDP calculated with the convolution approach. The biggest contributor to the SBO CCDP is the sequence probability of the scenario in which the AAC DG fails to start and the TDP becomes unable to operate owing to battery depletion ($P_{AS,BD}$), followed by the sequence probability of the scenario in which the AAC DG fails to run and the TDP becomes unable to operate owing to battery depletion ($P_{AR,BD}$).

4.2. Effect of modifying TDP mission time from T_m to T_{bd}

In Section 3.4, modifying the TDP mission time in the ET/FT approach from T_m to T_{bd} is discussed. Fig. 6 compares the numerical results for the three approaches when the suggested modification is performed. In the ET/FT approach, significant portions of $P_{AS,TR}$ and $P_{AR,TR}$ move to $P_{AS,BD}$ and $P_{AR,BD}$, respectively. Now, the ratio of $P_{AS,TR}$ and $P_{AR,TR}$ using the ET/FT approach with modified TDP mission time and the convolution approach reduces from 9.21 to 9.28 to only 1.63 and 1.65, respectively. This implies that the portions of $P_{AS,TR}$ and $P_{AS,TR}$ in the ET/FT approach was due to the conservative assignment of the TDP mission time. The overestimation of $P_{AR,BD}$ most significantly contributes to the overestimation of the CCDP when using the ET/FT approach with the modified TDP mission time.

The $P_{AS,TS}$ and $P_{AS,BD}$ calculated using the ET/FT approach with the modified TDP mission time are the same as those calculated using the convolution approach. The other four sequence probabilities that involve fail-to-run failures ($P_{AS,TR}$, $P_{AR,TS}$, $P_{AR,TR}$ and $P_{AR,BD}$) determined by the ET/FT approach with the modified TDP mission time are still conservative. By realistically modeling the time dependencies, the convolution approach eliminates unnecessary overestimation when fail-to-run failures are involved. The modification of the TDP mission time renders the ET/FT approach more consistent with the convolution approach (as well as the Monte Carlo simulation results).

The CCDP determined by the ET/FT approach with the modified TDP mission time, i.e., the sum of the six sequence probabilities, is now 1.42E-2, which is slightly less than that of the conventional ET/FT approach.

5. Conclusions

SBO risk is one of the most significant contributors to nuclear power plant risk. In this paper, the mathematical formulas for the sequence probabilities determined by the convolution approach are compared with those determined by the conventional ET/FT approach. One of the findings of the comparison revealed a new modeling improvement in the ET/FT approach, in which the battery depletion time of a TDP should be used as the mission time of a TDP.

The numerical results of the convolution approach are in good agreement with those of the Monte Carlo simulation, and provide an exact contribution of each sequence to SBO risk. The biggest contributor to the SBO CCDP is the sequence probability of the scenario in which the AAC DG fails to start and the TDP becomes unable to operate owing to battery depletion (71.37%), followed by the sequence probability of the scenario in which the AAC DG fails to run and the TDP becomes unable to operate owing to battery depletion (22.06%).

The numerical comparison also provides new insight into the conservativeness of the conventional ET/FT approach. The biggest contributor to the SBO risk overestimation determined by the ET/FT approach is the overestimation of the sequence probability of the scenario in which the AAC DG fails to run and the TDP becomes unable to operate owing to battery depletion.

The selection of an overly conservative TDP mission time in the ET/FT approach results in a significant difference between the ET/FT and convolution approaches. By modifying the TDP mission time with the battery depletion time, the sequence probabilities of the ET/FT approach become more consistent with those of the convolution approach.

The proposed framework for the systematic sequence identification and mathematical modeling of SBO risk is expected to contribute to the development of more detailed mathematical modeling for accident sequences with time dependencies in nuclear power plants. Additionally, the new insights into the conservatism of the conventional ET/FT approach and the proposed modeling improvement are expected to enhance the modeling and estimation of SBO risk.

Funding

This work was supported by the Nuclear Safety Research Program of the Korea Foundation of Nuclear Safety funded by the Korean Government's Nuclear Safety and Security Commission [grant number 2203027-0122-CG100, 2104028-0222-SB120].

Declaration of competing interest

The authors declare that they have no known competing financial interests or personal relationships that could have appeared to influence the work reported in this paper.

References

[1] Office of the Federal Register, Station Blackout (10 CFR 50.63), Code of federal regulations, June 1988.
[2] USNRC, Station Blackout (Regulatory Guide 1.155), United States Nuclear Regulatory Commission, Washington, DC, 1988. August.
[3] R.E. Battle, D.J. Campbell, Reliability of Emergency AC Power Systems at Nuclear Power Plants (NUREG/CR-2989), United States Nuclear Regulatory Commission, Washington, DC, 1983.
[4] A.M. Kolaczkowski, A.C. Payne Jr., Station Blackout Accident Analyses (NUREG/CR-3226), United States Nuclear Regulatory Commission, Washington, DC, 1983.
[5] P.W. Baranowsky, Evaluation of Station Blackout Accidents at Nuclear Power Plants (NUREG-1032), United States Nuclear Regulatory Commission, Washington, DC, 1988.
[6] S.A. Eide, C.D. Gentillon, T.E. Wierman, D.M. Rasmuson, Reevaluation of Station Blackout Risk at Nuclear Power Plants (NUREG/CR-6890), United States Nuclear Regulatory Commission, Washington, DC, 2005.
[7] IAEA, Case Study on the Use of PSA Methods: Station Blackout Risk at Millstone Unit 3, International Atomic Energy Agency, Vienna, Austria, 1991 (IAEA-TECDOC-593).
[8] J.A. Schroeder, R.F. Buell, Proposed SPAR Modeling Method for Quantifying Time Dependent Station Blackout Cut Sets, 10th International Probabilistic Safety Assessment & Management Conference (PSAM10), 2010.
[9] P.J. Rodi, Algorithms for Incorporation of Dynamic Recovery in Estimating Frequency of Critical Station Blackout, Master of Science Thesis, Texas A&M University, May 2012.
[10] J.K. Knudsen, T. Wood, S. Prescott, C. Smith, J.A. Schroeder, Convolution correction factor adjustments on static PRA models for event assessment, in: Proceedings of the International Topical Meeting on Probabilistic Safety Assessment and Analysis (PSA 2017), 2017, pp. 156–162.
[11] M.M. Degonish, Practical Application of the loss of offsite power recovery analysis using the convolution methodology, PSA2019, in: Proceedings of the International Topical Meeting on Probabilistic Safety Assessment and Analysis, 2019.
[12] M.C. Kim, Systematic approach and mathematical development for conditional core damage probabilities under station blackout of a nuclear power plant, Reliab. Eng. Syst. Saf. 217 (January 2022), 107969.
[13] KEPCO and KHNP, APR1400 Design Control Document, Tier 2 (APR1400-K-X-FS-14002-NP), Revision 3, Korea Electric Power Corporation (KEPCO) and Korea Hydro & Nuclear Power Co, Ltd. (KHNP), 2018.
[14] S.A. Eide, T.E. Wierman, C.D. Gentillon, D.M. Rasmuson, C.L. Atwood, Industry-average Performance for Components and Initiating Events at U.S. Commercial Nuclear Power Plants (NUREG/CR-6928), United States Nuclear Regulatory Commission, Washington, DC, 2007.
[15] Z. Ma, T.E. Wierman, K.J. Kvarfordt, Industry-average Performance for Components and Initiating Events at U.S. Commercial Nuclear Power Plants: 2020 Update (INL/EXT-21-65055), Idaho National Laboratory, Idaho Falls, Idaho, 2021.
[16] S.A. Eide, C.D. Gentillon, T.E. Wierman, D.M. Rasmuson, Reevaluation of Station Blackout Risk at Nuclear Power Plants - Analysis of Loss of Offsite Power Events: 1986-2004 (NUREG/CR-6890), United States Nuclear Regulatory Commission, Washington, DC, 2005.
[17] N. Johnson, Z. Ma, Analysis of Loss-Of-Offsite-Power Events 2020 Update (INL/EXT-21-64151), Idaho Falls, Idaho National Laboratory, Idaho, 2021.